ACADEMIA ROMÂNĂ
Revue Roumaine de Chimie
http://web.icf.ro/rrch/

Rev. Roum. Chim.,
2020, *65*(2), 149-164
DOI: 10.33224/rrch.2020.65.2.04

PARAMETRIC STUDY OF HIGH TEMPERATURE WATER GAS SHIFT REACTION FOR HYDROGEN PRODUCTION IN AN ADIABATIC PACKED BED MEMBRANE REACTOR

Imed EDDI and Lemnouer CHIBANE*

Laboratoire de Génie des Procédés Chimiques (LGPC), Département de Génie des Procédés, Faculté de Technologie, Université Ferhat Abbas Sétif 1, 19000, Sétif, Algérie

Received September 15, 2018

In this work, a theoretical study of an adiabatic Pd-Ag tubular membrane reactor is carried out for hydrogen recovery by carbon monoxide upgrading. The process is conducted using the catalytic high temperature water-gas-shift reaction (HT-WGS) over an industrial Fe_2O_3-Cr_2O_3-CuO catalyst. Indeed, a parametric sensitivity study was done by using a non-isothermal mathematical model developed for this purpose. The Pd-Ag membrane reactor performance was obtained by numerical integration of the obtained model and the principal metrics used are the CO conversion and on H_2 recovery predicted in a large game of operating conditions. From the main obtained results, the following remarks can be drawn: except of gas hourly space velocity (GHSV) and H_2O/CO feed molar ratio, increasing the inlet temperature, inert gas flow rate and reaction pressure are beneficial for achieving a higher hydrogen permeation rates. This leads to favor the H_2 production and resulting in the enhancement of CO conversion and of H_2 recovery with high purity. Finally, it was found that a near complete CO conversion (99.99%) and a high H_2 recovery (96.4%) can be achieved by combination of the obtained optimum operation conditions.

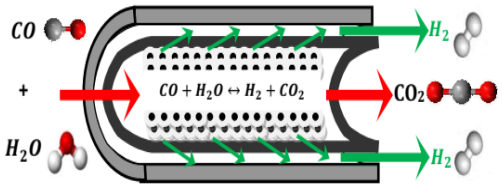

INTRODUCTION

The water-gas shift (WGS) reaction has been applied since a long time for syngas processing,[1] it is largely occurs commonly with steam reforming of hydrocarbons or partial oxidation of oil and natural gas.[1-2] Considering the single WGS reaction, the products mixture is mainly composed of H_2 and CO, CO_2, H_2O and small amounts of unconverted reactants.[3-4] Its major roles in various industrial applications are the production of hydrogen, which can be utilized as a clean fuel for use in gas turbines and fuel-cells and for ammonia synthesis in the fertilizer industry. It can be used also to adjust the CO/H_2 ratio as required for alternative hydrocarbon fuels through Fischer-Tropsch synthesis.[1,5-7] Commonly, the up-grading of the hydrogen-rich gas stream is devoted to reduce the CO concentration up to the required levels (typically 3000-4000ppm), having the two main following goals: the first consists to increase the hydrogen production rate and the second one to purify the reformate stream. The water gas shift reaction described by eq. (1)[3] allows realizing both precedent aims. The reaction takes place over an appropriate catalyst in which the water in the form of steam is mixed with carbon monoxide to obtain hydrogen and carbon dioxide, according to the following reaction:

$$CO + H_2O \leftrightarrow H_2 + CO_2 \qquad \Delta H_{WGS} = -41 kJmol^{-1} \qquad (1)$$

* Corresponding author lchibane@yahoo.com

It is known that the WGS reaction is kinetically and thermodynamically limited because it is both a reversible and exothermic reaction. Therefore in the practical industry, WGS reaction is performed in a two-stage adiabatic reactor with intermediate cooling:[8] the first stage consists of a high-temperature shift (HTS: at 643-673K and 10-60 bar) and the second called the low-temperature shift (LTS: at 473K and 10-40bar), utilizing Fe_2O_3-Cr_2O_3 and Cu-ZnO-Al_2O_3 catalysts, respectively. The output stream from the second reactor is then directed to some hydrogen separation unit for its purification by pressure swing adsorption or by using cryogenic distillation.[8] The WGS reaction was mostly studied over several catalysts, especially over iron based catalysts, and over a large wide of operating conditions. So, the obtained performances are different from a case to another case study. The HTS is characterized by fast kinetics, but the final CO conversion is limited by equilibrium constituting a rigid limit for a conventional reactor as a "closed system". On the contrary, the LTS undergoes slow kinetics, but the thermodynamic limitation is much less severe than that of HTS.[9] This affirmation could be justified by the obtained performances such as the observed reaction rates achieved over different designed catalyst, and at various operating conditions. Concerning the reaction rates, for instance the obtained findings under various temperatures, at a total pressure of 1atm and a H_2O/CO molar ratio of 1, show that in the case of Fe_2O_3-Cr_2O_3 (powder) catalyst the observed rate at 773K (19.5 $mol.g^{-1}.s^{-1}$) was almost 9 times higher than the obtained at 623K (1.98 $mol.g^{-1}.s^{-1}$).[10] In other hand, running the HT-WGS reaction over 1%wt Rh/Fe_2O_3-Cr_2O_3 exhibit an observed rate of 30.8 $mol{\cdot}g^{-1}{\cdot}s^{-1}$ at 773K, which is almost 3 times higher than the obtained at 623K (9.90 $mol{\cdot}g^{-1}{\cdot}s^{-1}$). So, it can be concluded from these examples the observed reaction rates obtained in the case of 1% wtRh/Fe_2O_3-Cr_2O_3 were as fast as the obtained ones in the case of Fe_2O_3-Cr_2O_3. It was also reported for both cases of HT-WGS and LT-WGS carried out over 1 wt%Rh/ Fe_2O_3-Cr_2O_3 catalyst and under a feed molar ratio H_2O/CO of 1, it is often necessary to operate at higher temperatures catalysts (HTS) to achieve sufficiently high reaction rates.[10]

For improving the performance of WGS reaction, the implementation of catalytic membrane reactors (CMR) is very promoted.[3,11] This technology seems very interesting and promising due to the attractive possibility of realizing both reaction and gas separation/purification in the same apparatus.[12] During the reaction, a selective membrane removes continuously one of the products from the reaction mixture and shifting the reaction toward the formation of desirable products, making it possible to reach higher conversion. So, the use of a membrane reactor for reversible reaction may be suppresses the equilibrium limitations.[13,14] As a result, the amount of catalyst for a desired conversion level is reduced.[13,15–17] Therefore, the combination of hydrogen perm-selective membranes and the WGS reaction constitutes the basic concept of membrane reactor technology, which involves various synergistic benefits to replace the high temperature shift complexity.[9,18-20] For this purpose, the judicious choice of the membrane, the membrane reactor design and the operational parameters are the most important considerations in drawing a WGS membrane reactor. Hence, in this context a considerable research activity has been focused on integration of H_2 perm-selective membranes in WGS reaction, and various mathematical models and simulation studies have been developed to describe their behavior in terms of reaction conversion and hydrogen recovery. According to this trend, several process operating variables, such as feed and permeate pressure, operating temperature, membrane thickness and the inert gas fraction for hydrogen evacuation, have been analyzed.[21-22] Different approaches can be used to develop models aimed at investigating how membrane responses may change under the influence of several variables. The WGS-CMR reactor is naturally corresponding to two-dimensional system (2-D). In this configuration, the reaction gas mixture flow is axial, while the separation of H_2 through the membrane is radial; therefore, the concentration gradients are not negligible in both dimensions. Practically, a reasonable assumption can be made that no significant radial concentration gradient exists if the length of the reactor is much greater (>10 times) than the characteristic width of the catalyst bed. Under this assumption, the model is considerably simplified for a one dimensional (1D-) mathematical representation.[18,23-24] The majority of the investigations on the WGS reaction in membrane reactors is relatively related to the low-temperature (<623K) operation. A few reports involved with the high-temperature operation (673K).[9,25] Therefore, considerable efforts are done for developing robust H_2-permselective membranes suitable for high-temperature WGS operation. In particular, dense Pd-alloy membranes, zeolite membranes, carbon molecular sieve membranes and micro-porous amorphous silica-based membranes are the most used for this purpose.[25-26] Palladium and its alloys such as Pd-Ag and Pd-Cu present an infinite hydrogen permselectivities which

makes it possible to obtain pure hydrogen according to H_2-specific permeation mechanism called solution-diffusion.[14,27] However, the use of the Pd membranes is limited due to their costs, embrittlement that is caused by the structure modification due to the α–β phase transformation and significant reduction in permeance, especially in the presence of carbon monoxide owing to competitive surface chemisorptions.[14,28] By using Pd-alloy membranes, obtained by alloying the Pd with Ni, Cu, Au, Ru and, in particular, Ag can reduce the precedent drawbacks. For example, the role could be played by silver is explained by its electron donating behavior, that is being largely analogous to the one of the hydrogen atom in palladium. Furthermore silver and hydrogen atoms would compete for the filling of electron holes.[12,29-31] In fact, depositing a thin Pd-layer on a porous supports, such as the Pd–Ag alloy membranes show lower cost because of a lower content of palladium.[3,9,28,32] Many one-dimensional (1-D) models have been proposed to simulate the performance of WGS reaction in Pd-Ag membrane reactors.[11,33] The WGS reaction was described and studied through a 1-D isothermal and isobaric model[17] to simulate the HT-WGS in a Pd-Ag membrane reactor in the temperature range of 673-773K to assess the effects of the feed condition (example: H_2O/CO molar ratio and inlet temperature) on the CO conversion and H_2 recovery. Their results highlight that the 98.2% was the best CO conversion in which obtained at 723K and corresponding to 81.2% of hydrogen recovery. The WGS reaction was also studied using both a Pd-based membrane and a Pd/Ag-based membrane in a temperature range of 331-350°C.[34] In order to interpret the reaction experimental data, two mathematical models describing the system under isothermal conditions and considered an axial differential mass balance in terms of partial pressure for each chemical species were developed. Their findings show that a complete separation of hydrogen from the other gases of the reaction system was obtained. The simulation study and the experimental results show a satisfactory agreement and both highlight the possibility to shift towards 100% the conversion by using the Pd/Ag membrane operating under the investigation conditions. A one dimensional non isothermal model was developed and used to compare the performances of a Pd-Ag MR operating at high temperature,[35] and a traditional process consisting of two (high and low temperature) reactors for the WGS reaction. The following variables were studied: inlet temperature, feed pressure, H_2O/CO feed molar ratio, and space velocity. They found that with only one stage based on a Pd-alloy MR can replace the two sections of the traditional process.

The main objective of the present study is to develop a simplified model to understand the effects of several HT-WGS membrane reactor operational parameters on its performance to define the optimal operating ones. A novel window for hydrogen production from the water gas shift reaction is proposed, using high temperature to enhance the rate of reaction and employing a hydrogen separation membrane for the collection of the high purity hydrogen product by the immediate evacuation of hydrogen across the Pd-Ag membrane at the used temperatures and other investigated parameters.

Membrane reactor description

In this study, water gas shift reaction is carried out in a Pd-Ag membrane reactor packed with an industrial Fe_2O_3-Cr_2O_3-CuO catalyst.[36] The membrane reactor under study is shown in Fig 1. The reactants were fed into the tube side of the reactor, while hydrogen will permeate through the Pd-Ag membrane to shell side through a Pd-Ag membrane of a thickness of 50μm. An inert gas flow rate (F_I) is introduced into the shell side to collect the permeated hydrogen. The hydrogen permeation occurs if the partial pressure of hydrogen on the tube side is greater than the shell hydrogen partial pressure. So, a low-pressure, high-purity hydrogen permeate is recovered from the shell side. The study of the HT-WGS reaction is conducted under the simulation conditions and membrane reactor properties shown in Table 1.

Mathematical model

Among the proposed models in the literature, and to simplify the complexity of the reactor computations, the pseudo-homogeneous model that used in our study is only considering one-dimension and it can be served for understanding the reactor behaviors under the investigated conditions. It should be noted that the average predictions obtained using this model remains as a solid approach for reactors calculations especially for reactors integrating membrane for separation. This approach is based on the following main considerations, in which used for describing the reactor under study: The radial dispersion is negligible; the transport by plug flow in the axial direction is considered, temperatures gradients in the axial direction are taken into account and the external resistances are considered to be negligible.[39] The radial gradient in gases concentration is not considered due to the infinite homogeneity at the plug flow regime.[40] The porosity along the catalyst bed was

considered also constant. So the pseudo homogeneous reactor model is obtained by coupling of the obtained equation of mass balance with the heat balance equation, therefore it is possible to predict the axial temperature profile under non-isothermal conditions.[41] In the following, the governing equations are separately presented for each part of Pd-Ag membrane.

1. Governing equation in tube side

a) Reaction rate correlations

In this study, an empirical power law type rate expression [36] in which given by Eq. (2) is used to describe the reaction kinetics on the iron-chrome oxide high temperature shift catalyst:

$$R_{WGS} = k^0 \exp\left(-\frac{E_a}{RT}\right) P_{CO}^a P_{H_2O}^b P_{CO_2}^c P_{H_2}^d \left(1 - \frac{1}{K_{eq}} \frac{P_{CO_2} P_{H_2}}{P_{CO} P_{H_2O}}\right) \quad (2)$$

Where R_{WGS} is the WGS reaction rate, P_j is the partial pressure of species j, and a, b, c and d are the reaction order of CO, H_2O, CO_2, H_2, respectively. k^0 is the pre-exponential factor, E_a is the apparent activation energy, T is the absolute temperature and R is the universal gas constant. Finally, the temperature dependence of the thermodynamic equilibrium constant is defined as: [42]

$$K_{ep} = \exp\left(\frac{4577.8}{T} - 4.33\right) \quad (3)$$

The various kinetic parameters values of the used kinetic model are summarized in Table 2.

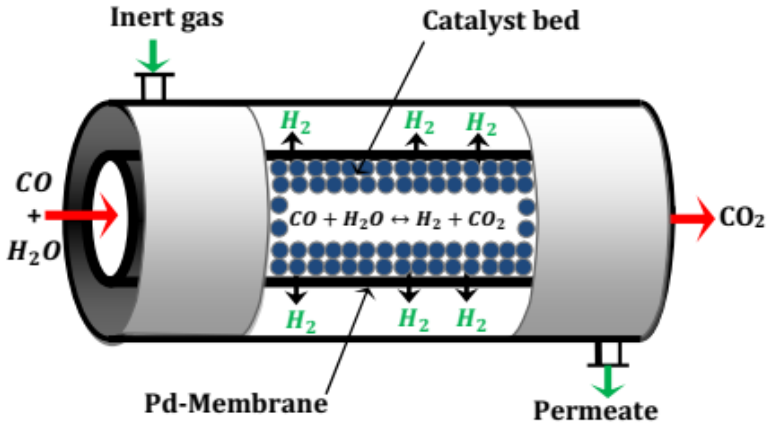

Fig. 1 – Schematic representation of Pd-Ag membrane reactor.

Table 1

Operating conditions, membrane properties and reactor dimensions

Parameters	**Values**	**References**
Total pressure, P_T	1-6 atm	9
Permeation pressure side, P_{perm}	1 atm	37
H_2O/CO feed molar ratio, φ	1-4	8,38
Gas hourly space velocity, $GHSV$	2000-6000 h^{-1}	8
Inert gas flow rate, F_I	50-150 mL min^{-1} of N_2	12
Catalyst bed porosity, ε	0.3	38
Catalyst Density, ρ_{cat}	7633.65 Kg m^{-3}	38
Pre-exponential factor, $Pe^0_{H_2}$	9.88×10^{-6} mol m^{-1} s^{-1} $kPa^{-0.5}$	8
Membrane activation energy, E	26.63 kJ mol^{-1}	8
Reactor length, L	5×10^{-2} m	38
Reactor diameter, D	15×10^{-3} m	38

Table 2

Kinetics model parameters[36]

Kinetic parameters		**Apparent reaction orders**			
k_0 *	E_a (kJ mol^{-1})	a $[CO]$	b $[H_2O]$	c $[H_2]$	d $[CO_2]$
-700	-111	1	0	-0.09	-0.36

*(molg(catalyst)$^{-1}$s^{-1}kPa$^{-(a+b+c+d)}$)

The partial pressures used for evaluate the WGS reaction rate in Eq. (2) are given by:

$$P_j = \frac{F_j}{F_T} P_T, \quad j = \text{CO, H}_2\text{O, CO}_2\text{, H}_2 \tag{4}$$

In the above equation, F_j is the molar flow rate of species *j*, P_T is the total pressure and F_T is the total molar flow rate in tube side defined as:

$$F_T = \sum F_j = F_{CO} + F_{H_2O} + F_{CO_2} + F_{H_2} \tag{5}$$

where F_{CO}, F_{H_2O}, F_{CO_2} and F_{H_2} are the molar flow rates of carbon monoxide, steam, carbon dioxide and hydrogen, respectively. Accordingly, the expression (5) can be rewritten as follows:

$$F_T = F_{CO}^0\left(1 + \varphi - Y_{H_2}\right) \tag{6}$$

where φ is the feed molar flow ratio defined as follows:

$$\varphi = \frac{F_{H_2O}^0}{F_{CO}^0} \tag{7}$$

where F_{CO}^0 and $F_{H_2O}^0$ are the inlet flow rate of carbon monoxide and steam at the reactor inlet, respectively. Finally, substituting Eq. (6) into Eq. (4), we obtain:

$$P_j = \frac{F_j}{F_{CO}^0\left(1 + \varphi - Y_{H_2}\right)} P_T \tag{8}$$

On other hand, the total molar flow rate in reactor inlet can be calculated:

$$F_T^0 = \frac{\left(\frac{Q}{3600}\right)}{22.4e-3} \tag{9}$$

where Q is the volumetric flow rate, which can be defined as:

$$Q = V \cdot GHSV \tag{10}$$

where V and $GHSV$ are the volume and the gas hourly space velocity, respectively. Thus, the total molar flow rate in reactor inlet is given by:

$$F_T^0 = F_{CO}^0 + F_{H_2O}^0 \tag{11}$$

b) Mass balance equation

The mass balances for each species on the tube side are given by Eq (12):

$$\frac{dF_j}{dz} = \rho_{cat}(1 - \varepsilon) A_C \sum_{i=1} \upsilon_{ij} R_i \tag{12}$$

where F_j is the molar flow rate of species j, z is the axial coordinate, υ_{ij} the stoichiometry coefficients (i refers to the reaction and j to the species), R_i is the reaction rate, A_C is cross-sectional area of tube side, ρ_{cat} is the catalyst density and ε is the catalyst bed porosity. After some mathematical arrangements and by introduction of a dimensionless length (ζ) to (eq. 12), we get:

$$\frac{dX_{CO}}{d\zeta} = \frac{\rho_{cat}(1 - \varepsilon) A_C L}{F_{CO}^0} R_{WGS} \tag{13}$$

2. Governing equation in shell side

As previously mentioned, the mass balance in shell side concerned only the hydrogen. The eliminated hydrogen through the Pd-Ag membrane is given by the following equation:

$$\frac{dF_{H_2}^{perm}}{dz} = A_m J_{H_2} \tag{14}$$

In the above equation, $F_{H_2}^{perm}$ is the hydrogen flow rate in the permeate side, A_m is the surface area of membrane and J_{H_2} is the permeation rate of hydrogen, given by the Fick-Sieverts law:[29]

$$J_{H_2} = \frac{Pe_{H_2}}{\delta}\left(P_{H_2,ret}^{0.5} - P_{H_2,perm}^{0.5}\right) \quad (15)$$

where Pe_{H_2} is the hydrogen permeability, $P_{H_2,ret}$ and $P_{H_2,perm}$ are the hydrogen partial pressures in retentate and permeate sides, respectively. δ is the membrane thickness. The dependence of the membrane permeability on the temperature can be expressed by the Arrhenius law: [29]

$$Pe_{H_2} = Pe_{H_2}^{0} \exp\left(\frac{-E}{RT}\right) \quad (16)$$

where $Pe_{H_2}^{0}$ and E are the pre-exponential factor and activation energy of hydrogen permeability, respectively.

$$J_{H_2} = \frac{Pe_{H_2}^{0}}{\delta} \exp\left(\frac{-E}{RT}\right)\left(P_{H_2,ret}^{0.5} - P_{H_2,perm}^{0.5}\right) \quad (17)$$

Therefore, according to the definition of the parameter Y_{H_2} as the ratio of hydrogen flow rate over the initial carbon monoxide flow rate, the differential equation can be written:

$$\frac{dY_{H_2}}{dz} = \frac{A_m}{F_{CO}^{0}} . \frac{Pe_{H_2}^{0}}{\delta} \exp\left(\frac{-E}{RT}\right)\left(P_{H_2,ret}^{0.5} - P_{H_2,perm}^{0.5}\right) \quad (18)$$

By introducing the dimensionless form, we get:

$$\frac{dY_{H_2}}{d\zeta} = \frac{\pi d_m L}{\delta F_{CO}^{0}} . Pe_{H_2}^{0} \exp\left(\frac{-E}{RT}\right)\left(P_{H_2,ret}^{0.5} - P_{H_2,perm}^{0.5}\right) \quad (19)$$

The hydrogen partial pressure in permeate side can be given:

$$P_{H_2,perm} = \frac{Y_{H_2} P_{perm}}{Y_{H_2} + I} \quad (20)$$

where I is the ratio between the molar inert gas flow rate (F_I) to the molar inlet carbon monoxide flow rate, defined as:

$$I = \frac{F_I}{F_{CO}^{0}} \quad (21)$$

3. Heat balance

The heat balance in the tube side with the adiabatic assumption can be simplified as follows[6]:

$$\frac{dT}{d\zeta} = \frac{(-\Delta H_{WGS}) R_{WGS} \rho_{cat} (1-\varepsilon) A_C L}{\sum Cp_j F_j} \quad (22)$$

where ΔH_{WGS} is the molar enthalpy of WGSR and Cp_j is the specific heat of species j given as follows: [6]

$$\frac{Cp_j}{R} = A + B_j T 10^{-3} + C_j T^2 10^{-6} + \frac{D_j}{T^2} 10^5 \quad (23)$$

Table 3

Specific heat capacities constants of species [6]

Cp_j	A	B	C	D
H_2	27.01	3.508	0	0.69
CO_2	45.369	8.688	0	9.619
CO	28.068	4.631	0	0.258
H_2O	28.849	12.055	0	1.006

The constants A, B, C, and D for each species are reported in Table 3.

Correspondingly, the heat balance in term of molar enthalpy is a function of the temperature T according to the following equation:

$$\Delta H_i(T) = \Delta H_T^{\circ} + \sum_j \nu_{i.j} \int_{T_{ref}}^{T} Cp_j^i(T).dT \ , \ T_{ref} = 298.15K \tag{24}$$

where ΔH_T° is the molar enthalpy of reaction at the standard state. T_{ref} is the reference temperature. Thus, by combining equations (24) and (25), the temperature dependence of the molar enthalpy of WGS reaction can be given by the following equation:

$$\Delta H_{WGS} = \Delta H_T^{\circ} + \sum_j \nu_j \int_{T_{ref}}^{T} \left(A_j + B_j T 10^{-3} + C_j T^2 10^{-6} + \frac{D_j}{T^2} 10^5 \right).dT \tag{25}$$

$$\Delta H_{WGS} = \Delta H_T^{\circ} + \sum_j \nu_j \left(A_j (T - T_{ref}) + \frac{B_j}{2} 10^{-3} (T^2 - T_{ref}^2) + \frac{C_j}{3} 10^{-6} (T^3 - T_{ref}^3) - D_j 10^5 \left(\frac{1}{T} - \frac{1}{T_{ref}} \right) \right) dT \tag{26}$$

Carbon monoxide conversion (X_{CO}) and hydrogen recovery (Y_{H_2}) are the evaluated performance of the Pd-Ag membrane reactor for conducting the HT-WGS reaction. These parameters are calculated according to equations (27) and (28), respectively:

$$X_{CO} = \frac{(F_{CO})_{in} - (F_{CO})_{out}}{(F_{CO})_{in}} \tag{27}$$

$$Y_{H_2} = \frac{F_{H_2}^{Perm}}{(F_{CO})_{in}} \tag{28}$$

where $(F_{CO})_{in}$, $(F_{CO})_{out}$ are the molar flow rate of carbon monoxide at the inlet and the outlet reactor, respectively. $F_{H_2}^{Perm}$ is the molar flow rate of hydrogen permeate in the shell side.

4. Numerical solution strategy

The literature indicates that it is desirable to perform WGSR at low temperature to obtain high CO conversion. However to achieve sufficiently high reaction rates, it is often necessary to operate at higher temperatures, even though the equilibrium composition is not so favorable under such conditions.[10,42,43] Therefore, CO conversion is thermodynamically favored by low temperatures but, on the contrary, its kinetics is promoted by a high temperature.[44] It is known that the HT-WGS is characterized by limit for the CO equilibrium conversion, so for overcome this constraint, removing hydrogen from the WGSR zone can break the equilibrium limitation and shifts the reaction toward the formation of products, making it possible to reach higher conversion. Based on these considerations, it should be noted that the equilibrium conversion are not presented in this work, and therefore it is limited to the evaluation of the CO conversion rates in the used membrane reactor, the quantities of hydrogen recovered and the temperature profiles under several operating conditions. These metrics are predicted from the obtained ordinary differential equations describing the behavior of the tube and shell sides. These equations are solved numerically using 4th order Runge–Kutta algorithm performed on MATLAB software with the following initial conditions at the reactor inlet: $T=T_0$, $X_{CO}=0$ and $Y_{H_2}=0$.

RESULTS AND DISCUSSION

In this section, the obtained results and their associated discussions are presented. Let's remember that the main purpose of the established numerical model is to use it as a main tool to maximizing the reactor performance by finding the optimum range of operating parameters. The effects of these parameters upon model performance are of the utmost importance, because the HT-WGS reaction output depends strongly on the combination of these operating parameters. Therefore, a parametric sensitivity analysis was carried out to investigate the influence of the following operating parameters: H_2O/CO feed molar ratio (1:1 to 4:1), inlet reaction

temperature (T_0: 350-500°C), inert gas flow rate (F_I : 50-150 mL/min of N_2), gas hourly space velocity (GHSV: 2000-6000 h^{-1}) and initial reaction pressure (P_0: 1-6 atm).

1. Effect of the feed molar ratio H_2O/CO

The study of the reactants molar fraction effect on the WGS-MR performance is of great importance. Therefore, the effect of steam content in the feed (steam to carbon monoxide ratios) on performance of Pd-Ag MR conducting the HT-WGS reaction was evaluated by varying the H_2O/CO molar ratio between 1 and 4 at the inlet temperature range from 350°C to 500°C, while keeping all other parameters fixed. The main results presented in Figs. 2 (a) and (b) show the obtained performance in terms of CO conversion and H_2 recovery, respectively. By analyzing Fig. 2(a), it was possible to see that before the inlet temperature of 410°C, the CO conversion increases significantly with increasing H_2O/CO molar ratio. For example, under the inlet temperature of 350°C, the CO conversion improved from 29% to 34% as the H_2O/CO molar ratio increased. It was therefore concluded that higher H_2O/CO ratios leads to higher CO conversions because the kinetics was favored for higher steam content. Besides, since the excess of H_2O shifts the WGS reaction toward the desirable products. In addition, it was usually recommended to avoid carbon formation in which may be caused by carbon monoxide dispro-portionation *via* the Boudouard reaction. This is leads to carbon deposition on the catalyst and as a result causes the catalyst deactivation.[37] On the other hand; more steam addition in the WGS reaction will cause higher energy consumption in its vaporization.[45] Therefore, a lower H_2O/CO molar ratio was favorable to reduce the amount of steam needed to achieve reasonable levels of CO conversion. However, above the inlet temperature of 410°C, further increase of H_2O/CO molar ratios results in a relatively slightly increase of CO conversion. Although, the CO conversion increases sharply in this inlet temperature range, this corresponds to a substantial increase in hydrogen production. A possible clarification is that less hydrogen was separated as illustrated in Fig. 2(b), when the inlet temperature increases from 410°C to 500°C. It was seen that a particular behavior was observed with increasing the H_2O/CO ratios; the hydrogen recovery shows a decrease trend. Particularly, the H_2 recovery decrease from 54% to 43%. Based on this observation, it was suggested that the water evaporation reduces the partial pressure of H_2 at the tube side, which decreases the hydrogen permeation driving force intervening in the H_2 solution-diffusion mechanism across the membrane. However, at the lower H_2O/CO molar ratio and for a given total pressure, the partial pressure of steam is reduced, and consequently the partial pressures of gaseous species including H_2 increase.[37] As a result, H_2 permeation rates are promoted by lowering H_2O/CO ratios and higher H_2 recovery were achieved. From point of view both CO conversion and H_2 recovery, the H_2O/CO molar ratio of 1:1 is appropriate. Regarding the axial temperature profiles (Fig. 2(c)) that obtained at different values of H_2O/CO molar ratios in the used inlet temperature range, it can be concluded that under the investigated conditions, the use of an inlet temperature higher than 470°C could provoke an undesirable increase in the reaction temperature in the whole system. This increase can lead to other undesirable phenomenon such as thermal instability, catalyst deactivation and reactor runaway. Based on these results, it is very recommended to carry out the HT-WGS reaction under temperatures below 470°C.

2. Effect of the reaction inlet temperature

To evaluate the dependence of the Pd-Ag MR performance on the reaction inlet temperature and feed pressure, the effect of the inlet reaction temperature on CO conversion and H_2 recovery was studied for 1, 3 and 6 atm. The optimum performance the HT-WGS reaction conducted in Pd-Ag MR should balance a high CO conversion and a high hydrogen recovery. As shown in Fig. 3(a), both CO conversion and H_2 recovery increase with the reaction inlet temperature increasing. In particular, it was interesting to notice that for the lower inlet temperatures below 410°C, the CO conversion is low of approximately 64%, because of the relatively slow reaction rate, and, consequently, the amount of H_2 produced was also small. Besides, the permeation of H_2 through Pd-Ag membranes was an activated process [46] therefore; H_2 recovery was not favored when operating in this inlet temperature range, so the equilibrium shift promoted by the H_2 recovery from the reaction medium was small about 29%. As the inlet temperature increases from 410°C to 500°C, CO conversion increases from 82% to 99% and H_2 recovery increases significantly from 40% to 54%. This was attributed to the reaction kinetics and the H_2 permeation rates were favored at this range of temperatures, since they follow an Arrhenius law. Therefore, higher H_2 permeation rate through the membrane making possible a

greater H_2 recovery in the shell side and promoting a higher CO conversion. However, in these operating conditions with the aim to improve even further greatly enhancing the hydrogen permeation rate to achieve high H_2 recovery by increasing the inlet reaction temperature from 410°C to 500°C may be difficult. In addition, the hydrogen permeation rate was not very high under the atmospheric pressure from where; the feed pressure was increased up to 3atm. As shown in Fig. 3(b), a very high CO conversion was close to 99.99% and significantly increase of H_2 recovery about 84% were achieved with the inlet temperature above 430°C. Moreover, under the pressure of 6atm as shown in Fig. 3(c), an extremely high H_2 recovery of 92% can be reached with temperature above 410°C. This results show that the reactor should be operated under high feed pressure by controlling the reaction temperature to achieve an increment of the hydrogen permeation driving force, resulting in the improvement of CO conversion and H_2 recovery. Furthermore, the optimum inlet reaction temperature for the current process was observed at 450°C in as much as this temperature yields the highest CO conversion and thereby high H_2 production. The axial temperature profiles were also presented for each inlet temperature as shown in Fig. 3(d). It was obtained that running the reaction with inlet temperatures between 470°C and 500°C are not recommended. According to the obtained results showing that the evolution of temperature in the whole system and regarding the temperatures required by HT-WGS, in the following, it was adopted that the reactor performances are preferably predicted at inlet temperatures ranged between 350°C and 450°C. Therefore, in the following the evolution of temperature was examined and presented for all cases study between 350°C and 450°C.

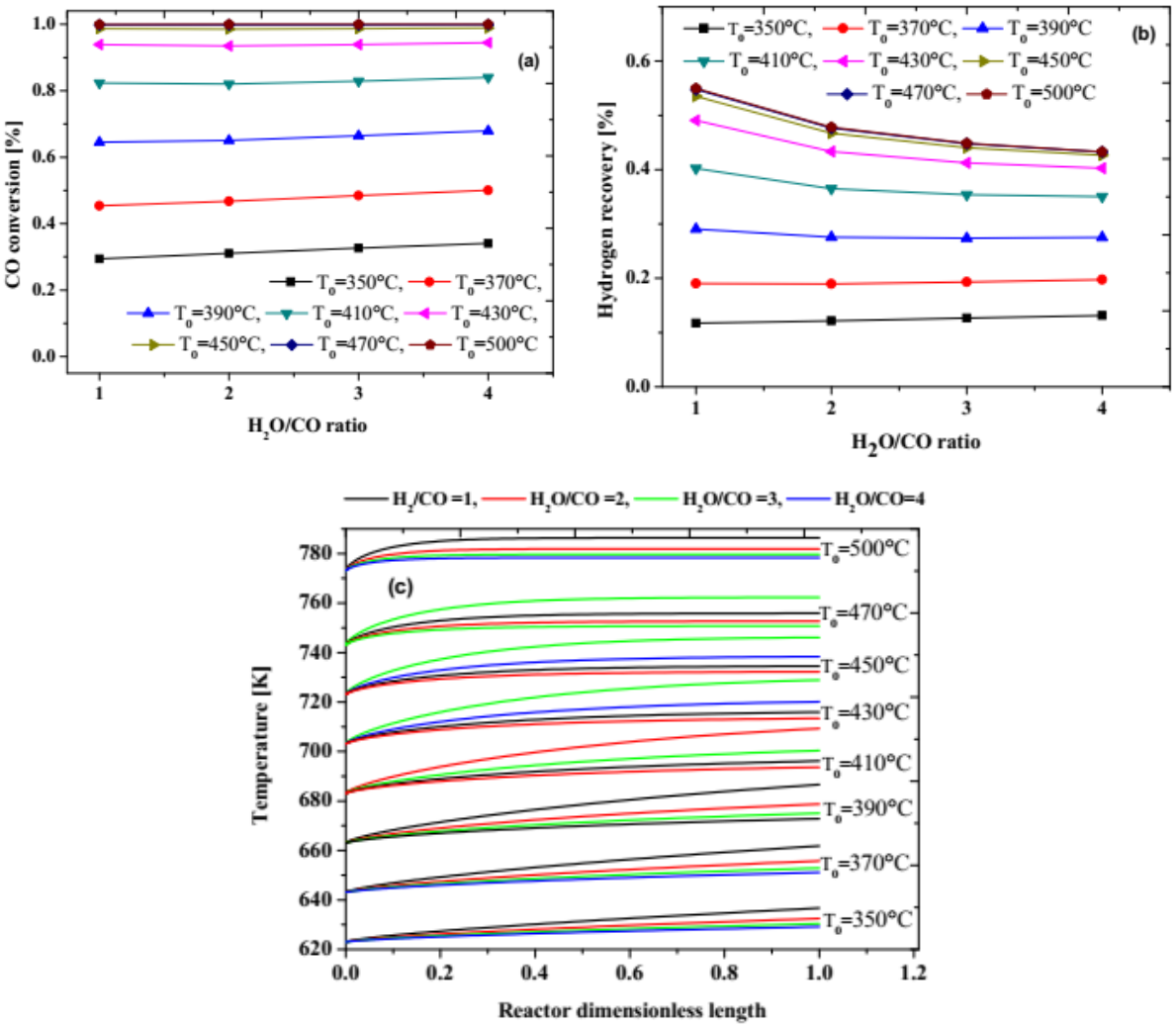

Fig. 2 – Reactor performance at different H_2O/CO molar ratio and different inlet temperatures: (a): CO conversion, (b): H_2 recovery, (c): axial temperature profile. Conditions: P_0 = 1atm, F_1 = 50 mL/min, GHSV = 2000h^{-1}.

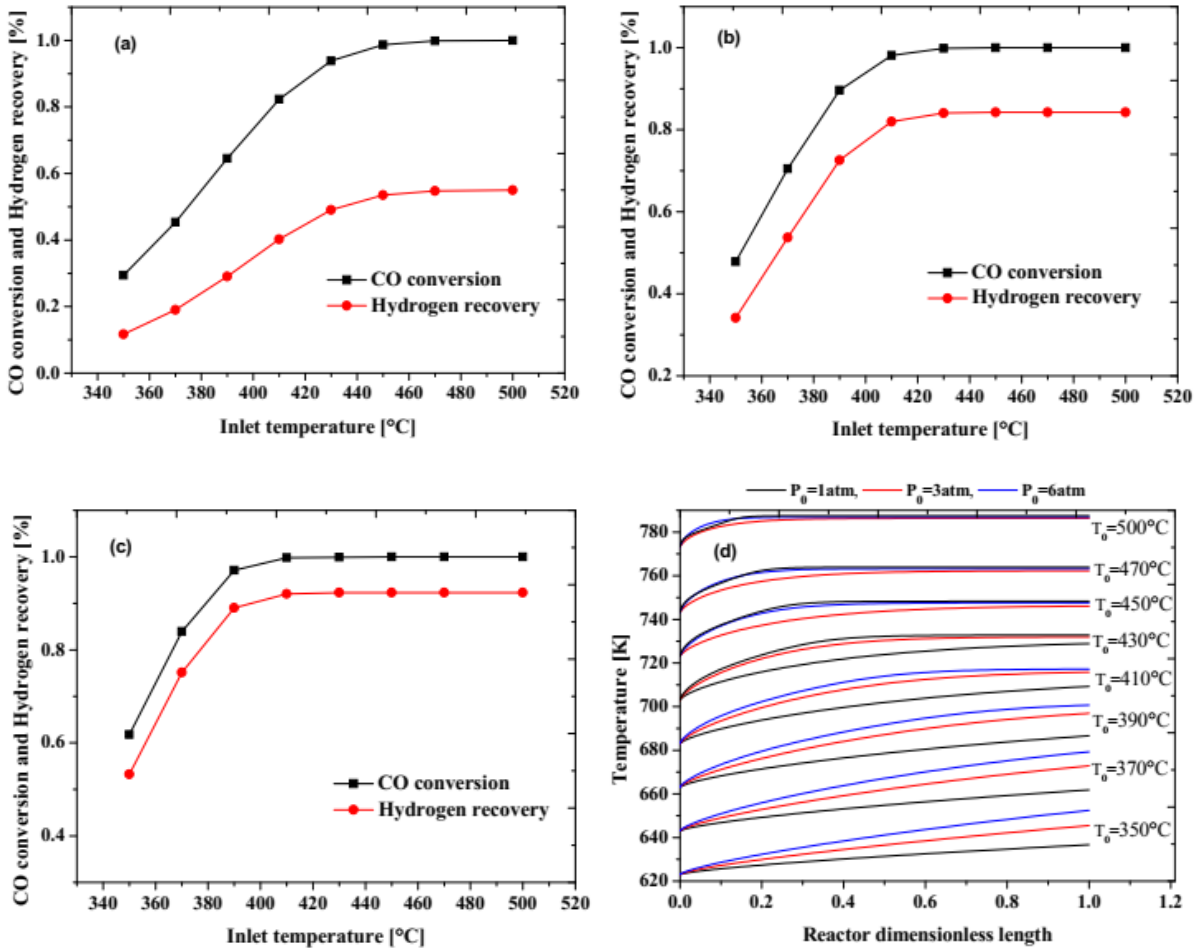

Fig. 3 – Reactor performance at different inlet temperature and at different initial total pressures:
(a): CO conversion and hydrogen recovery for P_0=1atm, (b): CO conversion and hydrogen recovery for P_0 = 3 atm,
(c): CO conversion and hydrogen recovery for P_0=6atm, (d): axial temperature profiles.
Conditions: F_I = 50 mL/min, GHSV = 2000 h^{-1}, H_2O/CO feed molar ratio = 1/1.

3. Effect of inert gas flow rate (F_I)

In general, it is important to achieve high hydrogen permeation rates for a successful application of Pd-Ag MR in the WGS reaction. However, the hydrogen partial pressure of the shell side was a limiting factor for H_2 production. Therefore, an effective way to achieve a higher hydrogen recovery is by decreasing the shell chamber pressure by applying vacuum to the shell side, or by applying an inert-gas.[46] In the current study, the effect of the inert gas (N_2) flow rate on the shell side of the Pd-Ag MR was evaluated. The results presented in Figs. 4 (a) and (b) show the obtained performance in terms of CO conversion and H_2 recovery, respectively. The main results show that as the inlet temperature increased from 350°C to 450°C, it can be seen that both CO conversion and H_2 recovery increase when the inert gas flow rate was increased from 50mL/min to 150mL/min. This may be explained by the positive effect of the inert gas flow rate for achieving high levels of H_2 recovery and CO conversion; this is achieved by the increasing of the hydrogen partial pressure difference between shell and tube sides according to Eq. (15). Therefore, the hydrogen partial pressure in the shell side decreases, in which implies a higher driving force for hydrogen permeation through the Pd-Ag membrane. So, the H_2 recovery was promoted and favors the CO consumption toward the products and conducting to reach higher conversions. In addition, the performances improvement are more evident when the system is operating at reaction temperature of 450°C, the increase of inert gas flow rate boost the H_2 recovery from 53% to 77% and enhancing the CO conversion from 98% to 99.31%. As result, it was possible to conclude that an inert gas flow rate is one of the key parameters in which can be used to maintain a higher hydrogen partial pressure

gradient across the Pd-Ag membrane, in favor of pure hydrogen recovery. Concerning the evolution of temperature as presented in Fig. 4(c), it appears that under the investigated conditions, the temperature changes gradually from the inlet up to the reactor exit. Herein, it should be noted that since the temperature profile does not exceed the required temperatures by HT-WGS reaction, it can be concluded that this inlet temperature of 450°C is safety and adequate for achieving a complete conversion and a higher amount of hydrogen recovery. Consequently, under adequate conditions of temperature and feed pressure, CO conversion and H_2 recovery could be widely promoted. It was possible to highlight that the fact that the use of an inert gas plays a more important role in the improvement of the CO conversion when the MR utilizes a membrane permselective to hydrogen. However, from an economic point of view the utilization of a large quantity of inert gas is not beneficial for industrial applications because an additional component was added to the system.[11]

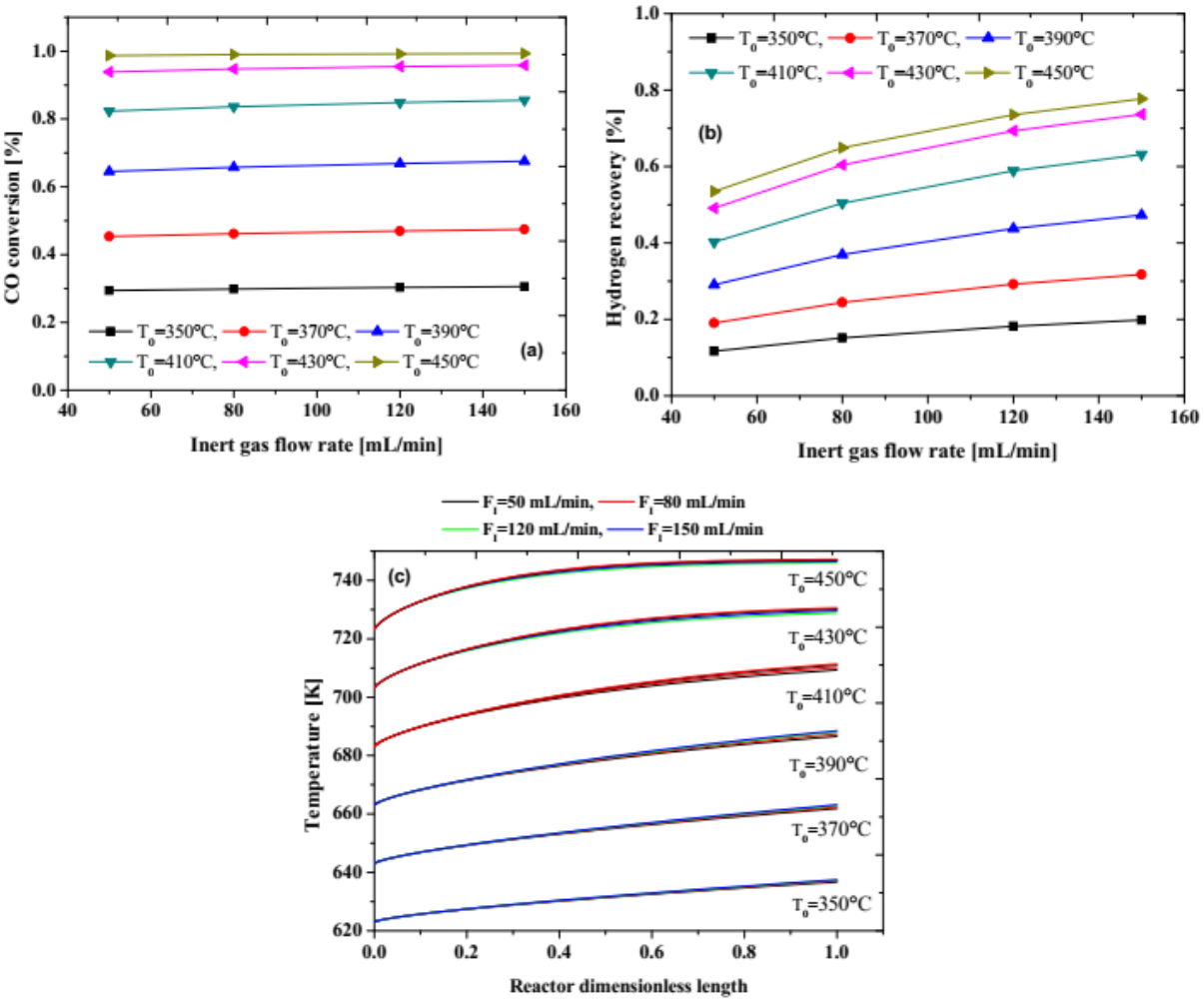

Fig. 4 – Reactor performance at different inert gas flow rates and for different inlet temperatures: (a): CO conversion, (b): hydrogen recovery, (c): axial temperature profiles. Conditions: P_0 = 1 atm, H_2O/CO feed molar ratio = 1/1, GHSV = 2000 h^{-1}.

4. Effect of GHSV

The effect of gas hourly space velocity (GHSV) on the HT-WGS reaction performance was also studied in a wide window from 2000h^{-1} to 6000h^{-1}, the inlet temperature was between 350°C and 450°C and the inert-gas flow rate was of 150mL/min. The main results of simulations in terms of CO conversion and H_2 recovery are shown in Figs. 5 (a) and (b), respectively. It is known that the GHSV is considered as a variable, which generally used to indicate the reverse of the residence time of reactants over a catalytic bed. Moreover a low GHSV indicates a high residence time and thus favors the conversion, whereas the contrary applies for a high GHSV. However, a

high GHSV is highly desirable since this means a low catalyst amount converts a high feed flow rate and a low reactor volume is required.[35] From Fig. 5(a) and (b), it was found that any increasing of GHSV causes a significant decrease on both CO conversion and H_2 recovery. For example, at an inlet temperature of 350°C, the CO conversion decrease from 30% to 13% and H_2 recovery decrease from 19% to 4% when the GHSV increased from 2000h^{-1} to 6000h^{-1}, respectively. However, further increase of the inlet temperature to 450°C, high CO conversion of 99% could be obtained. According to axial temperature profiles obtained under the investigated conditions (Fig. 5(c)), it can be reported that the obtained evolution of temperature does not exceed the allowed limits, which favors the use of this temperature. It was possible concluded that the higher GHSV affect negatively on CO conversion because reducing the residence time within the catalyst and the reactants inside the reactor, leading to the decrease of CO conversion. In addition, the depletion of CO conversion involves in a lower H_2 production and this determines a decrease of the H_2 permeation driving force with a consequent lower H_2 recovery in the shell side. Moreover, this negative effect was more pronounced for lower temperatures due to lower membrane permeability and higher sensitivity to CO poisoning and less favored kinetics which, leads to CO conversions bellow the equilibrium one. For this case, independently of the operating temperature lower GHSVs were always preferable for obtaining best performance.

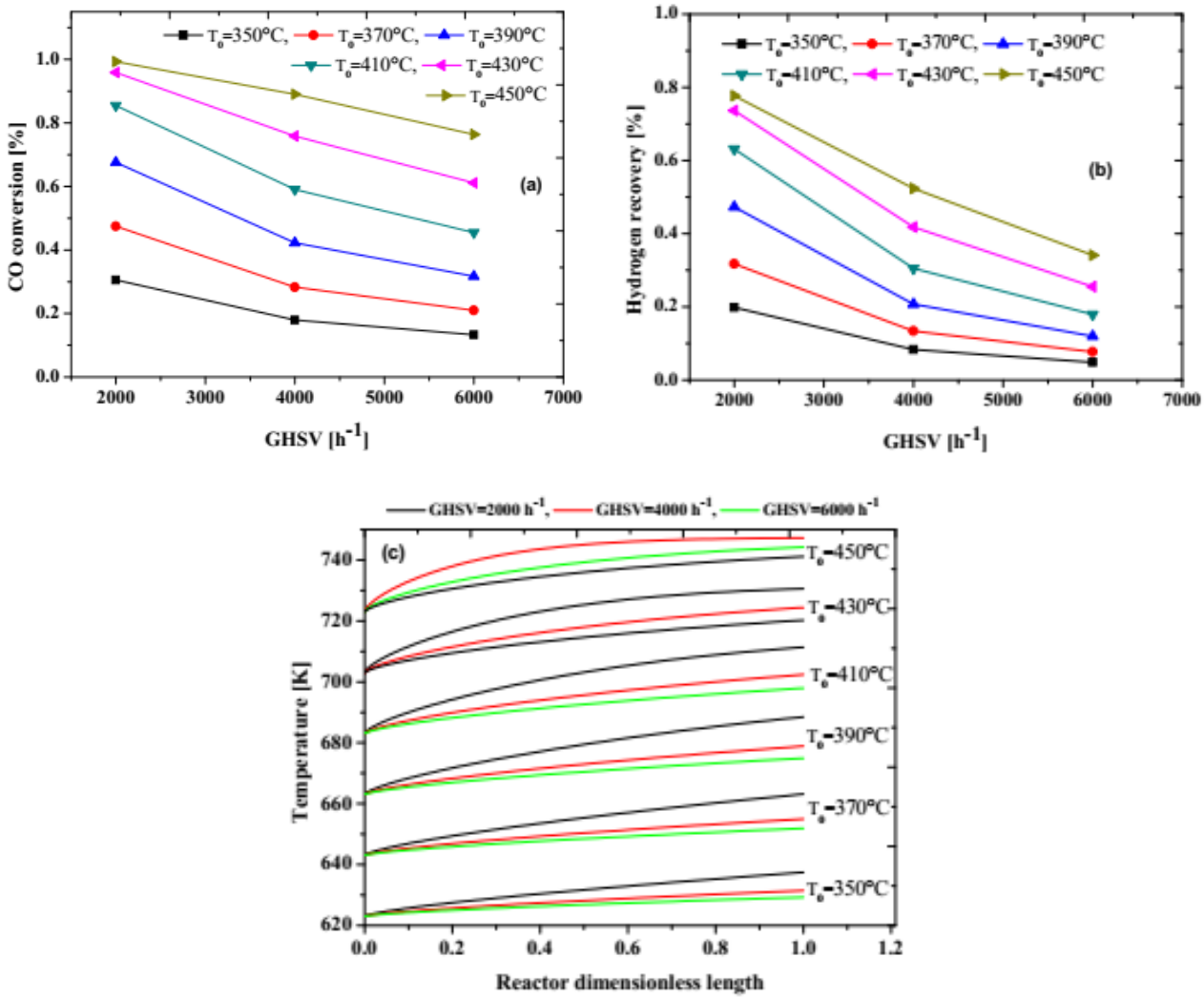

Fig. 5 – Reactor performance at different GHSV and at different inlet temperatures: (a): CO conversion, (b): hydrogen recovery, (c): axial temperature profiles. Conditions: P_0 = 1 atm, F_I = 150 mL/min, H_2O/CO feed molar ratio = 1/1.

5. Effect of the feed pressure

The effect of the feed pressure on the HT-WGS reaction performance carried out in Pd-Ag MR was studied by increasing this one from 1 to 6atm at inlet temperature of 350°C and 450°C. Fig. 6(a) and 6(b) shows the main results of simulations in terms of CO conversion and H_2 recovery as function of the feed pressure. As shown in Fig. 6(a) at T_0=350°C, it was clearly seen that when the feed pressure increases, both CO conversion and the H_2 recovery increases proportionally too. In fact, the feed pressure increase favors high hydrogen permeation. Thus, due higher H_2 recovery takes place, the carbon monoxide conversion may be enhanced. However, CO conversion was not improved too much as the operating pressure gets higher. In contrast, this increase was more evident as shown in Fig. 6(b), when the inlet temperature was 450°C, a nearly complete CO conversion was achieved, and the H_2 recovery changes from 77% up to 96.4%. Thus, our findings show that it was convenient to operate at higher pressure when the reaction was carried out at 450°C. Therefore, the trans-membrane pressure difference was improved by an increment in the feed pressure, which increases the H_2 permeation rate through the membrane leads to an increase in the rate of reaction and as consequence it enhancing noticeably the CO conversion. Therefore, the combination of a high feed pressure and high temperature were promoted a higher kinetic rate and higher membrane permeance, leading to high H_2 production and permeation rate, resulting improvement on CO conversion and H_2 recovery. Finally, the best operating conditions of the studied Pd-Ag membrane reactor are 450°C and 6atm, leading a CO conversion of 99.99% and H_2 recovery of 96.4%. In addition, since the obtained eligible temperature evolution as shown in Fig. 6(c), it can be reported that the achieved performances under a temperature of 450°C are very hopeful for CO upgrading to pure hydrogen by HT-WGS reaction.

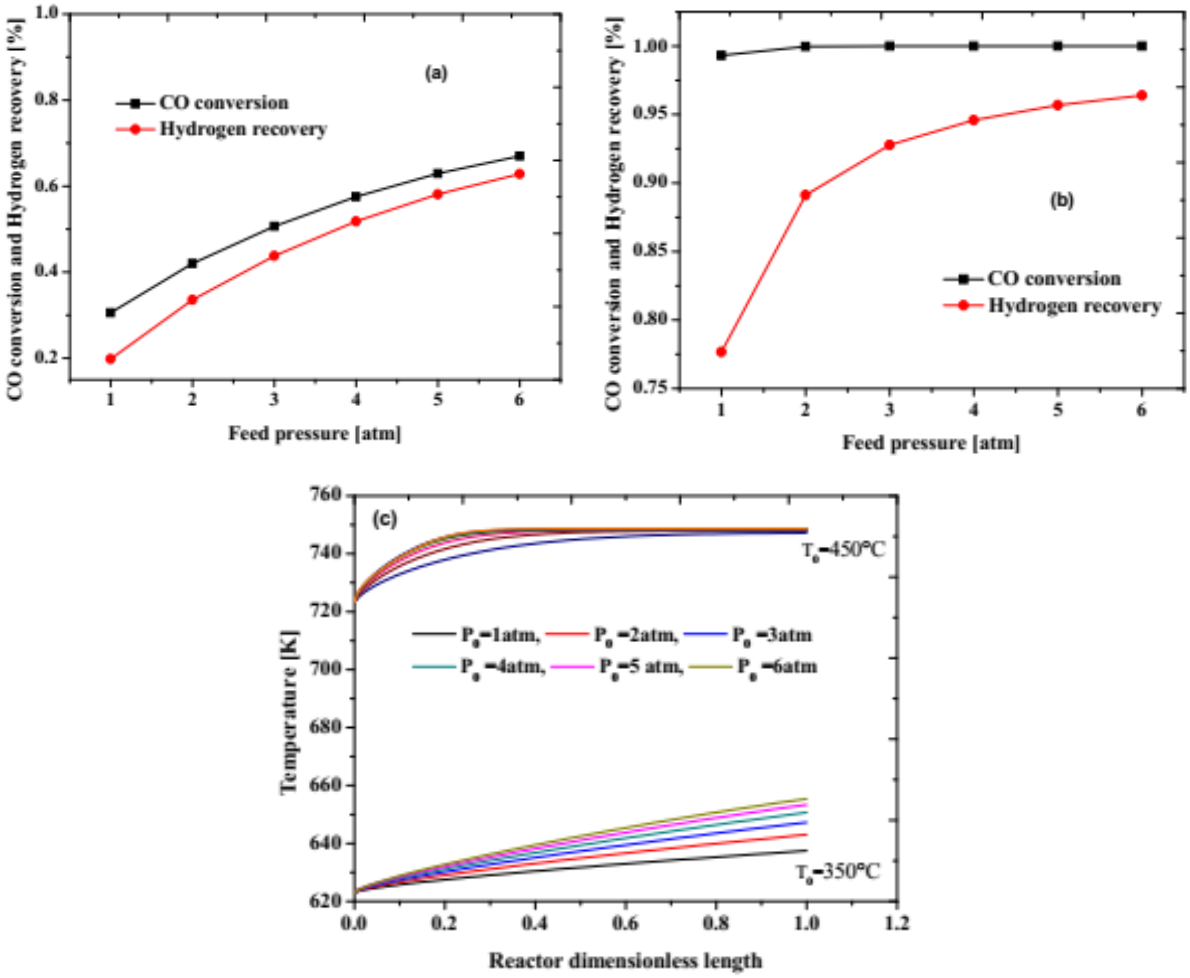

Fig. 6 – Reactor performance at different initial pressures and at different inlet temperatures: (a): CO conversion and hydrogen recovery at T_0 = 350°C, (b): CO conversion and hydrogen recovery at T_0 = 450°C, (c): axial temperature profiles at T_0 = 350°C and T_0 = 450°C. Conditions: H_2O/CO feed molar ratio = 1/1, F_1 = 150 mL/min, GHSV = 2000 h^{-1}.

CONCLUSION

In the current study, the performance of HT-WGS reaction carried out in a tubular Pd-Ag MR was numerically investigated using a one-dimensional adiabatic model developed for this purpose. In addition, a parametric study was established to optimize the process operation of HT-WGS membrane reactor. Therefore, H_2O/CO molar ratio, reaction inlet temperature, inert gas flow rate, GHSV and feed pressure are proved as key parameters to evaluate optimum operating conditions to maximize both CO conversion and H_2 recovery. According to our results and from carbon monoxide conversion point of view; it was found that the CO conversion depends strongly on the high temperatures and on feed pressure, while further increase of H_2O/CO molar ratio and inert gas flow rate resulted in only a slight improvement of CO conversion. Furthermore, it was found that an optimum reaction inlet temperature of 450°C was obtained in which the CO conversion was maxima. The effect of GHSV on the CO conversion was investigated and it was found that it affect negatively on CO conversion because reducing the residence time. A relatively low GHSV would be advantageous to CO conversion. Considering the H_2 recovery, higher reaction temperatures, feed pressure and inert gas flow rate show a positive effect, while higher H_2O/CO molar ratio and GHSV produce an opposite trend. It was also suggested that a low H_2O/CO molar ratio and GHSV were more suitable for high H_2 production and permeation rate through the Pd-Ag membrane to achieve high H_2 recovery.

According to the model prediction results, it can be suggested that the best performance of the Pd-Ag membrane reactor were obtained at $T_0 = 450$°C, $P_0 = 6$atm, GHSV = 2000 h^{-1}, $F_I = 150$ mL/min and H_2O/CO molar ratio = 1/1 with almost complete CO conversion and 96.4% of H_2 recovery. So, it can therefore be concluded that, the Pd-Ag WGS-MR is a promising system for high-purity hydrogen production for fuel cells applications. Finally, the developed model provides a valuable basis for evaluating reactors focused upon parametric sensitivity of operating conditions and H_2 separation rates, thereby reducing the experimental burden associated with catalytic membrane reactor development.

NOMENCLATURE

A_C – Cross-sectional area, m^2

A_j – Specific heat capacities constants of species j

A_m – Membrane surface area, m^2

B_j – Specific heat capacities constants of species j

C_j – Specific heat capacities constants of species j

Cp_j – Specific heat of species j, J mol^{-1} K^{-1}

D – Reactor diameter, m

D_j – Specific heat capacities constants of species j

d_m – Membrane diameter, m

E – Activation energy of hydrogen permeability, kJ mol^{-1}

E_a – Apparent activation energy, kJ mol^{-1}

F_j – Molar flow rate of species j, mol s^{-1}

F_T – Total molar flow rate in tube side, mol s^{-1}

F_{CO} – Molar flow rate of carbon monoxide, mol s^{-1}

F_{H_2O} – Molar flow rate of steam, mol s^{-1}

F_{CO_2} – Molar flow rate of carbon dioxide, mol s^{-1}

F_{H_2} – Molar flow rate of hydrogen, mol s^{-1}

F_T^0 – Total molar flow rate in reactor inlet, mol s^{-1}

F_{CO}^0 – Inlet flow rate of carbon monoxide, mol s^{-1}

$F_{H_2O}^0$ – Inlet flow rate of steam, mol s^{-1}

$F_{H_2}^{perm}$ – Hydrogen flow rate in the permeate side, mol s^{-1}

F_I – Molar flow rate of inert gas, mol s^{-1}

GHSV – Gas hourly space velocity, h^{-1}

J_{H_2} – Permeation rate of hydrogen, mol m^{-2} s^{-1}

K_{eq} – Thermodynamic equilibrium constant

k^0 – Pre-exponential factor, molg (catalyst)$^{-1}$$s^{-1}$$kPa^{-(a+b+c+d)}$

L – Reactor length, m

P_j – Partial pressure of gas component j, kPa

P_T – Total pressure, atm

P_{perm} – Permeation pressure side, atm

$P_{H_2,ret}$ – Hydrogen partial pressure in retentate, atm

$P_{H_2,perm}$ – Hydrogen partial pressure in permeate side, atm
Pe_{H_2} – Hydrogen permeability,
$Pe^0_{H_2}$ – Pre-exponential factor, mol $m^{-1}s^{-1}$ $kPa^{-0.5}$
Q – Volumetric flow rate, m^3s^{-1}
R – Universal gas constant, =8.314 J $K^{-1}mol^{-1}$
R_i – Reaction rate, mol $gcat^{-1}$ s^{-1}
R_{WGS} – Water gas shift reaction rate, mol $gcat^{-1}$ s^{-1}
T – Absolute temperature, K
T_{ref} – Reference temperature, K
V – Volume, m^3
X_{CO} – Carbon monoxide conversion
Y_{H_2} – Hydrogen recovery
z – Axial coordinate, m

Greek symbols

ΔH_{WGS} – Molar enthalpy of WGS reaction, J mol^{-1}
ΔH°_T – Reaction molar enthalpy at the standard state, J mol^{-1}
δ – Membrane thickness, m
ε – Catalyst bed porosity
φ – Feed molar flow ratio
ρ_{cat} – Catalyst density, kg m^{-3}
ζ – Dimensionless length,
υ_{ij} – Stoichiometric coefficient

Acronyms

CMR – Catalytic membrane reactor
HTS – High temperature shift
HT-WGS – High temperature-water gas shift
LTS – Low temperature shift
MR – Membrane reactor
WGSR – Water gas shift reaction

Subscripts

a – apparent
cat – catalyst
eq – equilibrium
i – reaction *i*
in – inlet of reactor
j – species *j*
m – membrane
out – outlet of reactor
perm – permeate side
ret – retenate side
ref – reference
T – Total

Superscripts

0 – Inlet conditions
a – Reaction order of carbon monoxide
b – Reaction order of steam
c – Reaction order of carbon dioxide
d – Reaction order of hydrogen

Acknowledgements. This work was supported in part by the University Ferhat Abbas Sétif 1, and the Ministry of Higher Education and Scientific Research (Algeria) with Project No.A16N01UN1-90120150009. Both institutions are gratefully acknowledged.

REFERENCES

1. S. S. Hla, G. J. Duffy, L. D. Morpeth, A. Cousins, D. G. Roberts and J. H. Edwards, *Catal. Commun*, **2009**, *11*, 272-275.
2. H. W. Haring, "Industrial gases processing", 1st edition, Weinheim, Wiley-VCH Verlag, 2008.
3. S. Liguori, P. Pinacci, P. K. Seelam, R. Keiski, F. Drago, V. Calabrò, A. Basile and A. Iulianelli, *Catal. Today*, **2012**, *193*, 87-94.
4. R. Y. Chein, Y. C. Chen, C. T. Yu and J. N. Chung, *Int. J. Hydrogen Energy*, **2015**, *40*, 8051-8061.
5. Y. Sun, S. S. Hla, G. J. Duffy, A. J. Cousins, D. French, L. D. Morpeth, J. H. Edwards and D. G. Roberts, *Int. J. Hydrogen Energy*, **2011**, *36*, 79-86.
6. E. Demirel and N. Ayas, *Theoretical Foundations Chem. Eng.,* **2017**, *51*, 76-87.
7. L. Chibane and B. Djellouli, *Int. J. Chem. Eng. App*., **2011**, *2*, 147-156.
8. A. Basile, S. Curcio, G. Bagnato, S. Liguori, S. M. Jokar and A. Iulianelli, *Int. J. Hydrogen Energy*, **2015**, *40*, 5897-5906.
9. A. Basile, L. Di Paola, F. I. Hai and V. Piemonte, "Membrane reactors for energy applications and basic chemical production", 1st edition, Wood head publishing, 2015.
10. Y. Lei, "Novel Fe_2O_3-Cr_2O_3 Catalyst for high temperature water gas shift reaction", *Dissertation*, University of New South Wales, **2005**.
11. P. Boutikos and V. Nikolakis, *J. Membr. Sci*., **2010**, *350*, 378-386.
12. D. Mendes, A. Mendes and L. M. Madeira, *Asia Pac. J. Chem. Eng*., **2010**, *5,* 111-137.
13. L. N. Baloyi, B. C. North, H. W. Langmi, B. J. Bladergroen and T. V. Ojumu, *South African J. Chem. Eng*., **2016**, *22*, 44-54.
14. E. L. Romero and B. A. Wilhite, *Chem. Eng. J*., **2012**, *207*, 552-563.
15. G. Chiappetta, G. Clarizia and E. Drioli, *Desalination*, **2006**, *193*, 267-279.
16. F. Gallucci, A. Basile and F. I. Hai, "Introduction - A review of membrane reactors", In "Membranes for membrane

reactors: preparation, optimization and selection", A. Basile and F. Gallucci (Eds.), United Kingdom: John Wiley & sons, 2011.
17. S. Tosti, F. Borgognoni, C. Rizzello and V. Violante, *Asia Pac. J. Chem. Eng*., **2009**, *4*, 369-379.
18. A. S. Augustine, Y. H. Ma and N. K. Kazantzis, *Int. J. Hydrogen Energy*, **2011**, *36*, 5350-5360.
19. A. Lotric, M. Sekavcnik, C. Kunze and H. Spliethoff, *J. Mech. Eng*., **2011**, *57*, 911-926.
20. M. Abdollahi, J. Yu, P. K. T. Liu, R. Ciora, M. Sahimi and T. T. Tsotsis, *J. Membr. Sci*., **2012**, *390-391*, 32-42.
21. W. H. Chen, C. W. Tsai, Y. L. Lin, R.Y. Chein and C. T. Yu, *Fuel*, **2017**, *199*, 358-371.
22. A. Caravella, F. P Di Maio and A. Di Renzo, *J. Membr. Sci*. **2008**, *321*, 209-221.
23. S. Kumar, S. Shankar, P. R. Shah and S. A. Kumar, *Int. J. Chem. Reac. Eng*., **2006**, *4*, 7-12.
24. G. Chiappetta, G. Clarizia and E. Drioli, *Chem. Eng. J*., **2008**, *136*, 373-382.
25. Z. Tang, S. J. Kim, G. K. Reddy, J. Dong, P. Smirniotis, *J. Membr. Sci*., **2010**, 354, 114-122.
26 J. Dong, Y. S. Lin, M. Kanezashi and Z. Tang, *J. Applied Physics*, **2008**, *104*, 121-301.
27. J. Catalano, M. G. Baschetti and G. C. Sarti, *J. Membr. Sci*., **2010**, *362*, 221-233.
28. A. Basile, F. Galluci and S. Tosti, "Synthesis, characterization, and applications of palladium membranes", in "Membrane Science and Technology", M. Reyes and M. Miguel (Eds.), 2008.
29. A. Basile, A. Iulianelli, T. Longo, S. Liguori and M. De Falco, "Pd-based selective membrane state of the art", in "Membrane reactors for hydrogen production processes", L. Marrelli, M. De Falco and G. Iaquaniello (Eds.), London, Dordrecht, Heidelberg, New York: Springer, 2011.
30. G. Q Lu, J. C. D da Costa, M. Duke, S. Giessler, R. Socolow, R. H. Williams and T. Kreutz, *J. Colloid Interface Sci*., **2007**, 314, 589-603.
31. T. Maneerung, K. Hidajat and S. Kawi, *J. Membr. Sci*., **2014**, *452*, 127-142.
32. A. Basile, F. Gallucci, A. Iulianelli, G. F. Tereschenko, M. M. Ermilova and N. V. Orekhova, *J. Membr. Sci*., **2008**, *310*, 44-50.
33. P. Marın, F. V. Dıez and S. Ordonez, *Int. J. Hydrogen Energy*, **2012**, *37*, 4997-5010.
34. A. Basile, G. Chiappetta, S. Tosti and V. Violante, *Separatio Purif. Techn.*, **2001,** *25*, 549-571.
35. G. Barbieri, A. Brunetti, A. Caravella and E. Drioli, *RSC Advances*, **2011**, *1*, 651-661.
36. S. S. Hla, D. Park, G. J. Duffy, J. H. Edwards, D. G. Roberts, A. Ilyushechkin, L. D. Morpeth and T. Nguy, *Chem. Eng. J.*, **2009**, *146*,148-154
37. L. D. Morpeth and M. D. Dolan, *Chem. Eng. J*., **2015**, *276*, 289-302.
38. W. H Chen, M. R Lin, T. L Jiang and M. H Chen, *Int. J. Hydrogen Energy*, **2008**, *33*, 6644-6656.
39. G. F. Froment, K. B. Bischoff and J. De Wilde, "Chemical reactor analysis and design", New York: Wiley, 1990.
40. Z. Rui, H. Ji and Y. S. Lin., *Int. J. Hydrog. Energy*, **2011**, *36*, 8292-300.
41. G. Maria, A. Marin, C. Wyss, S. Müller and E. Newson, *Chem. Eng. Sci*., **1996**, *51*, 2891-2896.
42. B. R. J. Smith and M. Loganathan, *Int. J. Chem. Reac. Eng*., **2010**, *8*, 7-13.
43. D. Vannier, "Kinetic study of high temperature water gas shift reaction", *Dissertation*, Norwegian University of Science and Technology, **2011**.
44. G. Barbieri, A. Brunetti, A. Caravella and E. Drioli, *RSC Advances*, **2011**, *1*, 651-661.
45. W. H. Chen, C. W. Tsai, Y. L. Lin, R. Y. Chein and C. T. Yu, *Fuel*, **2017**, *199*, 358-371.
46. D. Mendes, V. Chibante, J. M. Zheng, S. Tosti, F. Borgognoni, A. Mendes and L. M. Madeira, *Int. J. Hydrogen Energy*, **2010**, *35*, 12596-12608.